Through the looking-glass: microscopy techniques for studying mitochondria

Salvador Daniel Rivas Carrillo

Master's thesis

University of Turku

21.11.2022

Supervisor:

Nathaniel Street

UNIVERSITY OF TURKU

Salvador Daniel Rivas Carrillo:

Through the looking-glass: microscopy techniques for studying mitochondria

Master's thesis, 44 pp., 2 Appendices

November 2022

Abstract

Mitochondria are essential organelles of eukaryotic animal cells, representing the powerhouses fueling all cellular processes. Despite their fundamental importance for eukaryotic life, some aspects of their physiology remain obscure or poorly studied, partially due to technological limitations. For example: 1) transcellular degradation of mitochondria from one cell by another cell, transmitophagy, which has been observed in neurons and that is hypothesized to add to the known mechanisms of mitochondrial degradation, apoptosis and intracellular mitophagy; 2) the spatial association between Twinkle helicase, a protein indispensable for mitochondrial DNA replication, and mitochondrial-associated membrane structures, fatty-rich dynamic structures implicated in contact points with endoplasmic reticulum.

In this thesis, I collected more than 150 transmission electron microscopy images and established experimental parameters for fluorescence microscopy section of correlative light electron microscopy to study transmitophagy. Moreover, I established experimental parameters on sample preparation and staining when using fluorescence microscopy and immuno transmission electron microscopy with silver - nano gold coating to study mitochondrial DNA replication. Thus, this work aided in establishing experimental setups for available imaging techniques, which have added to the existing repertoire of tools to study mitochondria.

Keywords: Electron microscopy, mitochondria.

List of abbreviations

ATAD	ATPase family AAA domain-containing protein
ATP	Adenosine-5'-triphosphate
CLEM	Correlative light and electron microscopy
DMEM	Dulbecco's modified Eagle's medium
EM	Electron microscopy
ER	Endoplasmic reticulum
FACL4	Fatty acid-CoA ligase 4
LSM	Laser scanning confocal microscope
MAM	Mitochondria-associated membrane
MDS	Mitochondrial DNA depletion syndrome
MERC	Mitochondria - endoplasmic reticulum contact
MIB	Microscopy image browser
NADH	Nicotinamide adenine dinucleotide
NDI1	NADH dehydrogenase internal 1
PBS	Phosphate buffered saline
PEO	Progressive external ophthalmoplegia
ROS	Reactive oxygen species
STED	Stimulated emission depletion microscopy
TEM	Transmission electron microscope
TWNK	Twinkle helicase encoded gene
VDAC	Voltage-dependent anion channels
dsRNA	Double stranded RNA
mtDNA	Mitochondrial deoxyrribonucleic acid
mtRNAP	Mitochondrial RNA polymerase

Table of contents

1. Introduction

1.1. Mitochondria

Vision is a key sense of human kind. Vision has been one of our first, although not the most prominent, evolutionary successes. Therefore, it is only natural that vision would remain a key aspect in our quest for knowledge. As such, visually observing cellular organelles with help from technological advances in intact cells as well as perturbed conditions carries the potential to widen our understanding of the environment. In this thesis, I elaborate on the importance of observational technology, namely microscopy, in combination with other areas of research, for the study of cellular biology as applied specifically to mitochondria.

Mitochondria sit in an awkward spot in terms of cellular physiology. They are small organelles, ranging from 0.75 to 3 μm, with internal tubular structures of 28 nm diameter as shown in **Figure 1** (Frey and Mannella 2000). Mitochondria are often numerous, although their numbers are tightly correlated with the cell energy requirements. Yet mitochondria harbor their own circular DNA, similar to a prokaryotic organism, and their membrane complexity, vital for their physiology, loosely resembles that of unicellular organisms. Moreover, mitochondria are highly mobile and plastic, adjusting their size and shape as required, even performing fusion or fission (Kubli and Gustafsson 2012; Tilokani et al. 2018).

Apart from their energy supplier role, mitochondria serve other functions. For example: as a temporary short-term calcium storage and therefore regulator in the intracellular environment in vital cellular functions such as intracellular signaling and apoptosis; fuel consumption; lipid exchange (Baudier 2018; Szymański et al. 2017; Vance 2014). Furthermore, mitochondria have also proven a value asset for membrane biochemistry research since their independent machinery, capable of self-synthetizing proteins and lipids, can be manipulated and studied under different conditions (Horvath and Daum 2013).

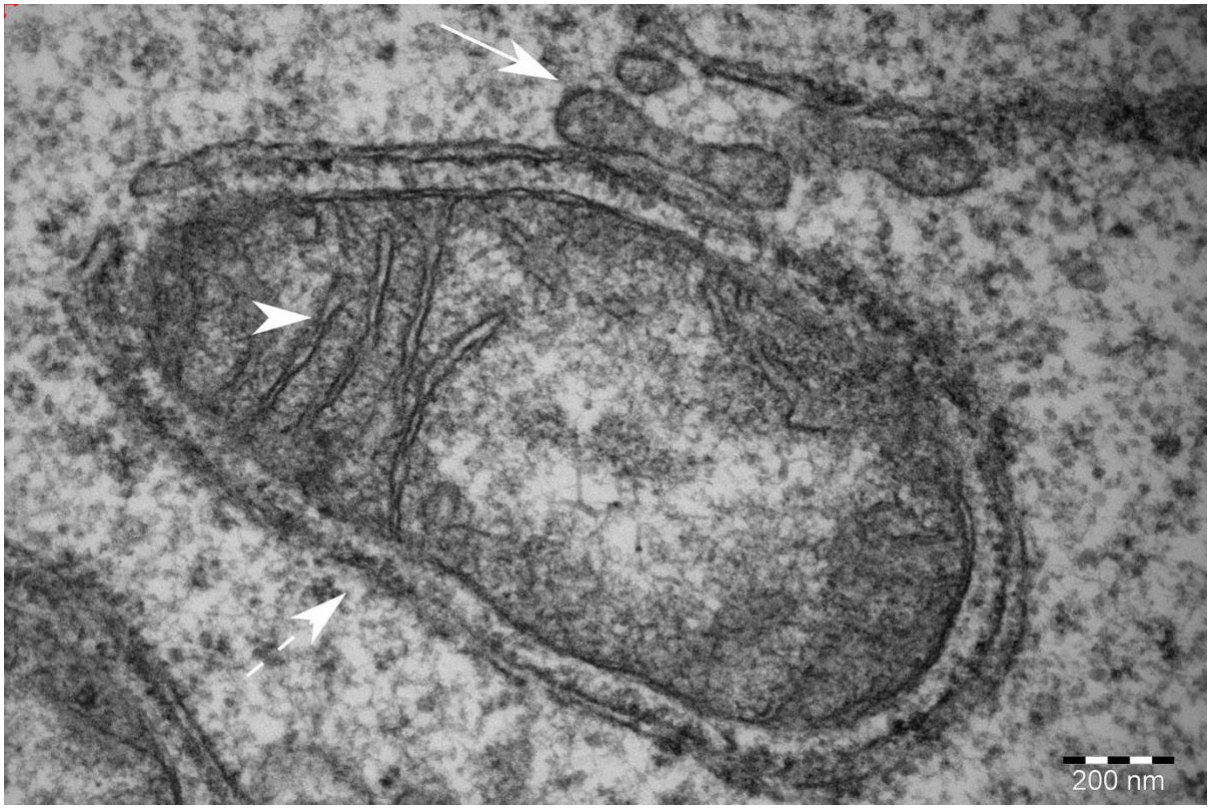

Figure 1. Human mitochondrion structure. The figure depicts transmission electron microscopy image of a human mitochondrion. The image show mitochondrial double external membrane (dashed arrow) as well as internal mitochondrial cristae (arrow head). Vesicle-like structures nearby the mitochondrial outer membrane are most likely endoplasmic reticulum (arrow), which demonstrates their tight interaction, see below.

Mitochondria produce most of the energy through the electron transport chain (see below). To fulfill this metabolic role, mitochondria have a specialized membrane organized into a double layer (Giacomello et al. 2020; Leal and Martins 2021). The outer mitochondrial membrane is permeable to ions and possesses voltage-dependent anion channels (VDAC), which serve as major transporters for metabolic products between the cytosol and the mitochondrial inter-membrane space, such as nucleotides, ions and other metabolites (Giacomello et al. 2020). In contrast, the inner membrane is folded onto itself to form cristae in order to maximize its surface (Frey and Mannella 2000; Cogliati, Enriquez, and Scorrano 2016; Ikon and Ryan 2017).

Moreover, the outer membrane can communicate with the endoplasmic reticulum (ER) by close juxtaposition through mitochondria-associated membrane (MAM) structures as illustrated in **Figure 2** (Vance 2014). It is now acknowledged that such junctions play an important role on the body homeostasis and alterations often lead to neurodegeneration (Szymański et al. 2017; Leal and Martins 2021)

The adoption of mitochondria, or whatever the origin might be, as the main energy supplier for cell metabolism has been tremendously successful from the evolutionary perspective. As such, they are almost ubiquitous in eukaryotic organisms. The fact that they function in a semi-independent and self-contained manner provides flexibility to adjust to a variety of environments. This flexibility is exemplified by hypoxic adaptation conditions, such as in embryonic stem cells, or during cell differentiation when an increased oxidative energy supply is required (Baudier 2018).

There are a number of methods available to study mitochondrial physiology, however morphological and physiological posse significant constraints, for instance mitochondrial localization in the intracellular environment, high redox states, double membrane architecture, among others. These constrains have impeded the study of different physiological mitochondrial processes, such as transmitophagy (Davis et al. 2014; Davis and Marsh-Armstrong 2014) and mitochondrial lipid-dependent DNA replication (Plucinska and Misgeld 2016). For these reasons, robust image methodologies to study mitochondrial physiology are required. In this thesis, I present a set of imaging techniques aimed at studying various aspect of mitochondrial morphology and physiology.

1.2. Mitochondrial degradation

In mitochondria, energy is produced by the electron transport chain. This chain is an intricate network of regulation, degradation and repair pathways that consists of a series of protein complexes whose function is to produce a transmembrane proton electrochemical gradient by redox reactions (Zhang et al. 2022; Małecki, Davydova, and Falnes 2022). This mechanim is ancient since it has been observed in many species across eukaryote species (Usey and Huet 2022). Sporadic dysfunction of the electron transport chain inevitably leads to accumulation of byproducts that can be extremely toxic to the cellular metabolism (Pereira and Beck-Da-Silva 2022; Dinicolantonio, McCarty, and O'Keefe 2022; Braga et al. 2022; Saravanan et al. 2022).

NADH dehydrogenase, also known as Complex I, is the largest component of the electron transport chain as well as its initiator. It is a sophisticated multi-subunit enzyme embedded on the mitochondrial inner membrane. Complex I has been identified as the main source of premature electron leakage, therefore a major contributor to superoxide production (see below) (Dang et al. 2020; Boveris and Cadenas 1975; Loschen et al. 1974; Babior 2004; Parey et al. 2020)

If mitochondria become quiescent organelles, this can lead to inefficient ATP production, generating reactive oxygen species (see below), lower the threshold for cytochrome c release, which in turn results in apoptosis (Stotland and Gottlieb 2015). To avoid this condition, cells keep control over mitochondria status via a process known as selective mitochondrial autophagy or mitophagy. This process disposes of dysfunctional or impaired mitochondria (Kubli and Gustafsson 2012; Ashrafi and Schwarz 2013; Cairns et al. 2020). On the other hand, mitochondrial biogenesis utilizes degradation products to assemble new organelles and insert them into the functional mitochondrial pool (Stotland and Gottlieb 2015). This mitochondrial cycle is a dynamic process occurring in parallel for many organelle units within one cell. An exception occurs in cardiomyocytes, where these events develop in a more static manner (Shirihai, Song, and Dorn 2015). Study of these degradation pathways is important due to their role in several diseases and aging (Shi, Guberman, and Kirshenbaum 2018) as well as diabetes type 2 and cancer (Rovira-Llopis et al. 2017; Williams and Caino 2018; Zorzano, Liesa, and Palacin 2009).

Reactive oxygen species (ROS) are oxygen derived free radicals and related oxidants. They occur ubiquitously and are characterized for being short-lived. These molecules take active part in redox reactions that lead to biomolecules modifications. However, ROS display particular affinity towards target proteins and lipids (Okamoto 2011). Mitochondria are the main source of ROS. Thus, maintaining control over redox status is essential for cell survival at all levels. For this purpose, cells harbor a broad repertoire of enzymatic and non-enzymatic mechanisms that aim at maintaining redox equilibrium and ROS control, i.e., fusion, fission, mitochondrial autophagy or mitophagy and mitochondrial biogenesis (Melser, Lavie, and Bénard 2015; Ni, Williams, and Ding 2015; Okamoto 2011; Okamoto and Kondo-Okamoto 2012; Tong and Sadoshima 2016). In spite of these systems, excess in oxidant formation, that causes accumulation of new products that compromise cell physiology, occur frequently (Radi 2018).

Previous research has indicated that transduction of the *NDI1* gene, which encodes internal NADH dehydrogenase from *Saccharomyces cerevisiae*, causes the inhibition of complex I and consequently generation of ROS (Pepe, Mentzer, and Gottlieb 2014; Seo et al. 2006; Yagi et al. 2001).

Recently, an alternative for mitochondrial degradation has been identified in neurons (Davis et al. 2014; Davis and Marsh-Armstrong 2014). However, the mechanisms and conditions under which this form mitochondrial degradation occurs, i.e., transmitophagy, remain unclear. To investigate this, I use imaging techniques to determine whether large vesicles produced in *NDI1* transduced cells could be used as markers for mitochondrial degradation. A visual summary of the known pathways of mitochondrial degradation can be found on **Figure 2**.

1.3. Mitochondrial replication

Besides energy production, mitochondria function as a fundamental regulator of cellular processes including import and assembly of their own proteins, direct transfer of lipids and steroid biosynthesis, cell calcium regulation, mitochondrial DNA maintenance. Hence, changes in mitochondrial stability lead to dramatic alteration of cell functions (Baudier 2018).

To accomplish these tasks, mitochondria hold, although ephemeral, close apposition with ER. Such connections are mediated by specialized fatty-rich dynamic membranes structures known as MAMs and mitochondria - ER contacts (MERCs). These structures are enriched in several lipid biosynthetic enzymes tethered to mitochondria. Moreover, they mediate lipid transport through the movement of vesicles. Alterations in such structures result in pathological states, which emphasizes their importance (Vance 2014). Furthermore, mitochondria are a major site for calcium storage. Release of calcium from ER occurs through ion channels that are highly concentrated in MAMs (Vance 2014).

Mitochondria contain their own DNA (mtDNA), which kept into one circular chromosome of 16 569 base pairs encoding only 37 genes (Young and Copeland 2016). Human mtDNA polymerase γ (pol γ) is a heterodimer that handles replication and repair of mtDNA. It is constituted of one 140-kDa catalytic subunit (p140) and one 110-kDa homodimeric subunit (p55) encoded by *POLG* and *POLG2*, respectively (Young and Copeland 2016). mtDNA forms complexes with a set of proteins that maintain their stability and are involved in replication, e. g. mitochondrial DNA helise Twinkle and mitochondrial DNA polymerase polG. These units are called nucleoids (Gerhold et al. 2015; Spelbrink 2009; Spelbrink et al. 2001).

The mitochondrial replicosome is composed of a number of proteins that function in synchrony with Pol γ: topoisomerase, mtDNA helicase Twinkle, mitochondrial RNA polymerase (mtRNAP), RNaseH1, mitochondrial single-stranded DNA-binding protein and mitochondrial DNA ligase III (Young and Copeland 2016).

Furthermore, it has been previously shown that Twinkle helicase is tightly associated with MAMs even in the absence of mtDNA, indicating their role in the membrane-associated replication platform (Gerhold et al. 2015; Spelbrink 2009; Spelbrink et al. 2001). Twinkle helicase encoded gene *TWNK* can wield missense mutation that co-segregate with other mitochondrial disorders (adult-onset PEO, hepatocerebral syndrome with MDS and infantile-onset spinocerebellar ataxia) (Young and Copeland 2016; Rajala et al. 2014).

Moreover, mitochondrial DNA nucleoids contain several proteins, such as ATPase family AAA domain-containing protein 3 (ATAD3). Mitochondrial DNA nucleoids are associated with MAM structures. In multicellular eukaryotes, ATAD3 is enriched and anchors MAMs as well as regulates dynamics of mitochondria - ER interactions (Gerhold et al. 2015). In

Hominidae, ATAD3 has been duplicated in tandem twice. This cluster is positioned on chromosome 1p36.33 (Merle et al. 2012). It seems that different ATAD3 are expressed at different times and sites. For instance, ATAD3B is expressed in human embryonic cells, whereas ATADA is characterized for its ubiquitous profile in all tissues at all stages of life. At the nucleotide sequence, the three versions of ATAD3 also differ. Such differences range from point mutations between ATAD3A and ATAD3B to ATAD3C lacking four exons, situation that might render it as a pseudogene (Baudier 2018). Defective ATAD3 versions have been characterized in pathological conditions (Murayama et al. 2019).

Mitochondrial replicative helicase, Twinkle helicase, encoded in *TWNK* gene can wield missense mutation that co-segregate with other mitochondrial disorders (adult-onset PEO, hepatocerebral syndrome with MDS and infantile-onset spinocerebellar ataxia) (Young and Copeland 2016).

Recent studies have indicated the involvement of ATAD3 on mtDNA replicating complexes and their relationship, direct or indirect, with ER via cholesterol-rich platform (Gerhold et al. 2015). Technical and biological difficulties, mitochondrial localization and membrane architecture, have limited the investigation, particularly on the spatial domain. Therefore, the relation and roles of FACL4 or ACSL4, a MAM maker protein, and Twinkle have not been entirely elucidated. A visual representation of the main biological components studied during this thesis can be found on **Figure 2**.

In order to investigate this relationship and set up experimental conditions for the methods used, I collected high-resolution fluorescence and immuno EM microscopy images from mitochondrial membrane proteins as well as established experimental parameters for immuno EM microscopy preparation.

Previous studies have suggested a model where mammalian mtDNA replicating complexes are directly or indirectly tethered to ER via a cholesterol-rich membrane platform, whose organization relies on ATAD3 (Gerhold et al. 2015). However, the relationship between FACL4, a MAM marker protein also known as ACSL4, and Twinkle has not been established, particularly in the spatial dimension.

To investigate this relationship, I collected high-resolution imagery of mitochondrial membrane proteins through fluorescence and immuno EM microscopy. Specific biological constrains, i.e., mitochondrial double membranes, render immuno staining for EM microscopy challenging.

1.4. Imaging techniques

Microscopy is the amplification of the field of vision by concentrating the light beams into the observer (Stockert 2017). Although this technique has been know to humanity for several centuries, recent times have witnessed significant improvements that have naturally benefited the application realms of such techniques. Considering that microscopy presents, beyond numerous applications, extensive accumulated knowledge I will only elaborate on a brief description of the methods used during this work, that is fluorescence microscopy, correlative light electron microscopy (Voortman 2014), super resolution microscopy (Patterson 2009; Lee et al. 2010; Bates et al. 2007; Huang et al. 2008), immuno electron microscopy (Anderson et al. 2018).

1.5. Fluorescence microscopy

Fluorescence microscopy improves onto this technique by utilizing fluorophores, molecules that react by absorbing light, falling into an excited state and emitting light of a different wavelength. In this manner, fluorophores can be conveniently used as spatial reporters during microscopy, which in combination with other biological processes, e.g., immunological reactions, nucleic acid amplification, synthesis or degradation of biochemical products, etc., can be adapted with ease.

Moreover, confocal microscopy uses the light source stimulation, in this case a laser beam focus over the sample and restricts capture of emitted light by a physical barrier, pinhole. In this manner, reducing the scatter light significantly, thus improving noise-signal ratio and therefore the image quality.

Fluorescence microscopy offers several advantageous features:

- Portability. Refereeing to the flexibility of confocal microscopy to be adapted to other biological or chemical experimental procedures, e.g., cell cultures, knock down or knock out genes, and other cell biology experiments.

- Scalability by automatization processes. This is possible because once the samples are prepared, and fluorophores added, automation can be implemented to allow capturing several hundreds of images in a run.

- Possibility to capture images *in vivo*. Due to the flexibility described above, it is possible to use a set of confocal microscopy techniques, although not all, to perform live imaging, which offers capturing on time domain and a closer resemblance to physiological conditions.

Reporter usage. Confocal microscopy uses light to record images. For this reason, it is possible to utilize physical phenomena to create reporters and attach them to desire molecules for identification. This set up is robust and reliable. For instance, usage of fluorophores in combination with immunological reactions, antibodies.

However, confocal microscopy also carries some limitations.

- Dependency on fluorophores. Identification of cellular structures is difficult on widefield microscopy due to poor resolution and large noise-signal ratio. An alternative is to use reporters to correct noise-signal ratio. However, the usage of reporters during confocal microscopy, i.e., fluorophores, limits the reporter space. In other words, the wavelength of the fluorophores can interfere with each other, cross-talk, creating noise. Moreover, reporter usage also creates observational bias by limiting the measurements to only reported phenomena.

- Resolution limitation. Confocal microscopy is a light-dependent technique, therefore it cannot, on the conventional sense, go beyond the light limit. There are a set of techniques specifically designed to improve on this problem, discussed below.

1.6. Super Resolution Light Microscopy

As mentioned above, light microscopy is constrained by the difraction limit. This problem has been addressed by the development of super resolution light microscopy techniques. Such techniques can be classified as deterministic and stochastic according to the procedure by which they collect information (Tam and Merino 2015; Vicidomini, Bianchini, and Diaspro 2018). Considering that during this thesis only I used Stimulated Emission Depletion (STED) (Hell and Wichmann 1994) among super resolution techniques, I will only expand upon this. But please bear in mind that other techniques exist and offer different advantages and disadvantages.

Conventional fluorescence excites an electron from the ground state into an excited electronic state of a different fundamental energy level. After relaxation to ground states, the excited fluorophore emits a photon. In STED, the excited electron relaxes forcely into a higher vibrational state. This process translates into two consecuences, a) the photon is realeased in a different wavelenght, and b) the electron transitions to a higher vibrational state with lowere energy in comparison to regular fluorescence. As a consecuence of the latter, the photon shifts farther away to the red spectrum by virtude of lowered energy and increased wavelenght. This change causes a difference between the two types of photons, and allows the stimulated to be ignored. In order to force this alternative emission, a photon must strike at the correct moment the fluorphore, thus the number of photons has a direct impact on emission efficiency and supression (Hell and Wichmann 1994; Hell 2003).

The main advantage and natural purpose of STED, and for all super resolution microscopy technique for that matter, is to improve resolution. However, this improvement comes at the cost of disadvantages including the use of more reporters, fluorophores, therefore restricting further the options in this dimension. Moreover, STED microscopy requires special equipment and maintenance that can be rather expensive (Hell 2003).

1.7. Electron Microscopy

Electron microscopes use a beam of accelerated electrons to iluminate an specimen and create an image. This system has a classic or conventional arrangement where the electron source is located on top as it flows downward to and throught the sample and the recorder is located on the bottom section. This set up is therefore called transmission electron micrscopy and used as a conventional term. Other set ups are available, however will not be discussed on this thesis.

The fact that electron microscopy uses electrons and not fluorophores circunvents the typical problem with light microscopy, as discussed above, along with other related issues. However, electron microscopy brings several disadvantages such as: high costs of equiment maintanance and sample preparation, although current light microscopes are comparable in maintanance budget; extensive and cumbersome process of sample preparation that often requires specialiazed personal in contrast with the relative straight forward methodology with other microscopy techniques; the impossibility to study live processes, mainly due to the lenghty sample preparation process.

1.8. Correlative Light Electron Microscopy

For the reasons listed above, alternatives that use the advantages of combinatorial techniques while reducing the disadvantages to the possible minimum are always actively seek. To combine light and electron microscopy, Correlative Light Electron Microscopy (CLEM) has been developed (Prabhakar et al. 2018). During this procedure, samples are recorded by light microscopy, usually confocal mounted on a gold nanoprinted ink printed coverslip. Next, the same sample is processed and prepared for electron microscopy where by utilizing the labels coordinates can be determined. Potential improvements on these techniques would be the use of image recognition algorithms, for example convolutional neural networks, to detect features and correlate coordinates with prior data. In this manner, creating an outer validation method that can correlate with internal validation, i.e., gold nanoparticle ink printed coverslip.

1.9. Immuno Electron Microscopy

As discussed above, the usage of reporters during signal collection significantly improves noise-signal ratio. A common, although no universal, practice during confocal microscopy is to take advantage of the strong and highly specific interaction between antibodies and antigens and attaching a reporter to the antibody's Fc region. By using this method, spurious biochemical binding is minimized, thus reducing false negative signal. However, usage of fluorophores during electron microscopy would not work since, as discussed above, signal depends on the density of the sample. Thus, the reporter during electron microscopy can be any material that surpasses the density of the sample, e.g., gold.

1.10. Summary

The work on this thesis contributed to the establishment of experimental parameters and collection of preliminary data on the study of mitochondria using the following imaging techniques:

- Transmission electron microscopy on NDI1-expressing cells.
- Correlative Light Electron Microscopy on NDI1-expressing cells.
- Confocal and super resolution (STED) fluorescence microscopy of mitochondrial DNA nucleoid proteins, ATAD3 and FACL4.
- Immuno electron microscopy of ATAD3.

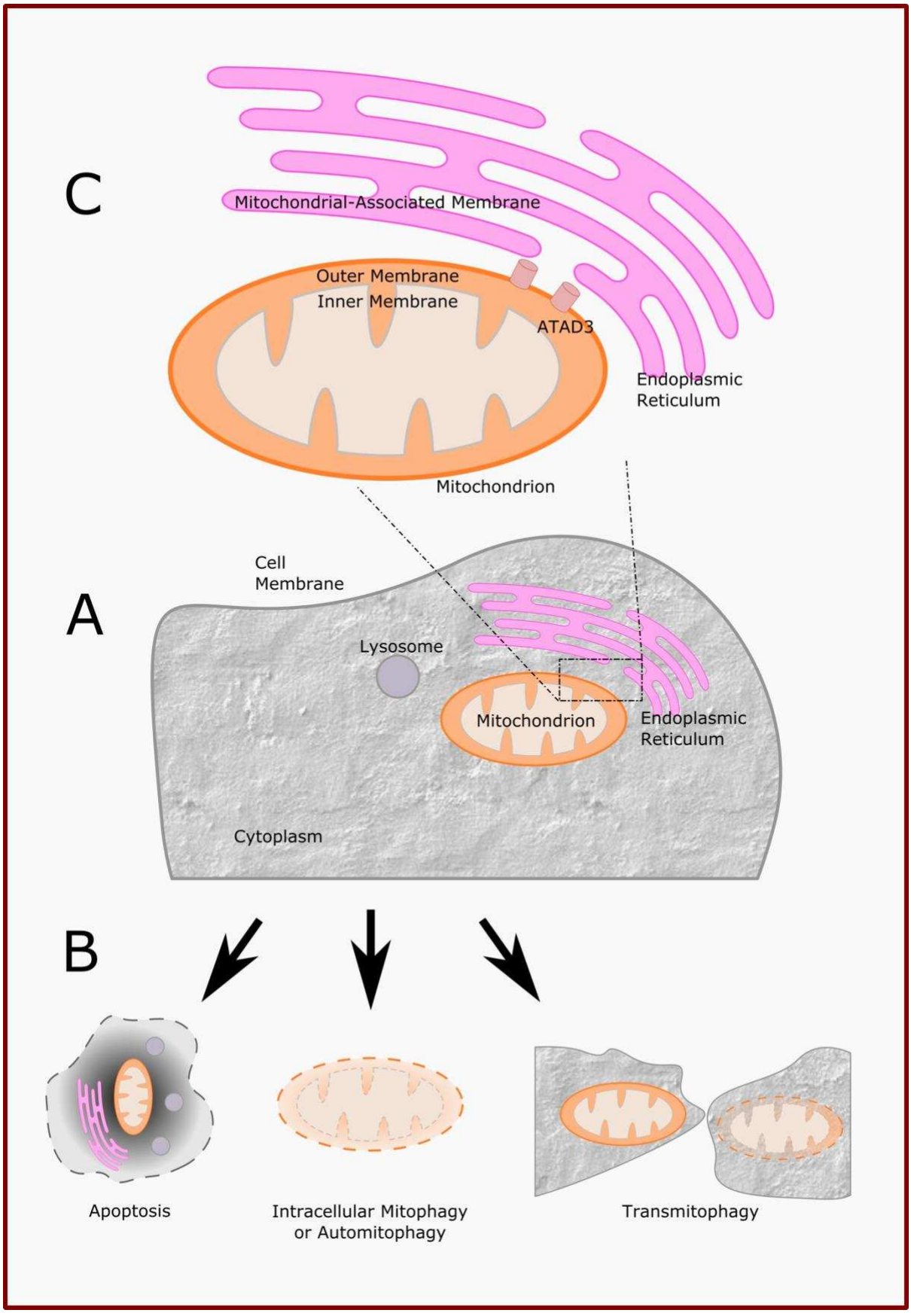
C
Mitochondrial-Associated Membrane
Outer Membrane
Inner Membrane
ATAD3
Endoplasmic Reticulum
Mitochondrion
A
Cell Membrane
Lysosome
Mitochondrion
Endoplasmic Reticulum
Cytoplasm
B
Apoptosis
Intracellular Mitophagy or Automitophagy
Transmitophagy

Figure 2. Schematic of the cellular processes describe in this thesis. **Panel A** illustrates an overview of the mitochondria in terms of cellular geography. As mentioned above, mitochondria number and morphology vary as a function of cellular demands and physiological conditions. **Panel B** shows biological pathway to degradate mitochondria. From left to right: 1) Apoptosis, a control cell death mediated by several intra and extracellular signal pathways. It involves degradative sub organelles, such as lysosomes. 2) Intracellular mitophagy or Autophagy, where quiescent mitochondria are targeted for degradation in the constrain of a cell. This process disposes and recycles mitochondria inside a cell. 3) Transmitophagy, where mitochondria are transferred from cell to cell via cellular protrusions, presumably for degradation, other subcellular processes might be involved. **Panel C** displays in detail Mitochondrial - Endoplasmic Reticulum contact sites. These subcellular structures are important for a variety of reasons, described in detail on the text. The illustration shows ATAD3 protein at the center of mitochondria - endoplasmic reticulum interaction. Other proteins and biomolecules are involved, not shown.

2. Aims

The aims of the current work include two main points:

First, to study mitochondrial degradation by: a) identifying cell to cell transfer of vesicle-like structures, which are positive for mitochondrial and lysosomal markers; and b) establishing experimental parameters for Fluorescence Microscopy section of Correlative Light and Electron Microscopy (CLEM) for vesicle-like structures positive to mitotracker.

Second, to study mitochondrial DNA replication by: a) identifying the presence of Twinkle helicase and FACL4 on the mitochondrial membrane by Fluorescence Microscopy; and b) establishing experimental parameters for silver coating for immuno Electron Microscopy for localizing ATAD3 on the mitochondrial membrane.

3. Materials and Methods

3.1 Cell culture

Human embryonic kidney cells from Invitrogen (cell line T-REx^{TM}- 293) were cultured at 37°C with 5 % of CO_2 in Dulbecco's modified Eagle's medium (Gibco 41966-029 inc. L-Glutamine and Pyruvate) supplemented with 1% Penicillin-Streptomycin antibiotics. The medium for wild type HEK cells was additionally supplemented with 10% fetal bovine serum (FBS). The medium for HEK cells with ATAD3B transgene was additionally supplemented with 10% Tetracycline free FBS, 15 µg ml^{-1} Blasticidin (Invitrogen) and 100 µg ml^{-1} Hygromycin (Invitrogen).

Cell line HEK293T was grown according to ATCC (http://www.lgcstandards-atcc.org/), in high glucose (4.5 g/l) at 37°C and 5% CO_2. To study cell physiology under conditions enforcing dependence on mitochondrial ATP production, cells were grown in glucose-free galactose (4.5 g/l) medium for 24 hours. Amino-acid starvation was induced by incubating cells in RPMI 1640 medium without amino acids (Sigma-Aldrich) for 45 minutes. Serum starvation was produced by incubating cells overnight in DMEM without fetal calf serum. For cell synchronization by double thymidine block, a 25% confluent cell population was exposed to 2 mM thymidine (Sigma-Aldrich) for 18 hours. The thymidine block was released by incubation in DMEM for 9 h. Synchronization in G2/M was obtained after a second exposure to 2 mM thymidine for 17 h. Upon the release from the thymidine block, the cells were cultured in DMEM in order to follow progression through the next cell cycle. For synchronization by aphidicolin, a 70% confluent cell population was blocked in G1/S phase using 2.5 µg/ml aphidicolin (AO781 Sigma) for 24 h. G2/M phase was reached culturing the cells in DMEM for 6-9 h after removal of the aphidicolin. Cell-cycle phase was determined by flow-cytometry analysis of cells stained with propidium iodide.

3.2 ATAD3 knock-down by RNAi

ATAD3 knockdown with RNA interference was done essentially as in (He et al., 2012). The dsRNA sequence used was 5'-UCAAUGAGGAGAAUUUACGGAAGCA-3' and 5'-UGCUUCCGUAAAUUCUCCUCAUUGA-3'. Cells were plated at 10% confluency in 100 mm and 35 mm cell culture dishes. After 24 h cells were washed once with optiMEM and for a single 100 mm dish 3 ml of optiMEM, 18 µl of Lipofectamine 2000 (Invitrogen) and 50 nM of siRNA was added for ATAD3 expression knockdown. Cells transfected with a scrambled, non-targeting siRNA (Negative control, Low GC duplex, Invitrogen) were used as controls. Samples were then incubated for 4 hours at 37°C after which 3 ml of cell growth media with 30% of fetal bovine serum was added to the 100 mm dishes. After 24 h of knockdown additional 4 ml of media was added to keep the cells growing in 10 ml of media. DsRNA transfection was repeated after 48 h of the first treatment.

3.3 Mitotracker and Lysotracker staining

MitoTracker Red (Invitrogen) and LysoTracker Blue (Life technologies) staining was performed on control HEK cells and cells treated with RNAi to reduce ATAD3 expression. First, 0.3% intermediate solution of LysoTracker in cell growth medium was made. The cells, grown on glass bottomed 35 mm dishes, were washed with 1 ml of growth medium before staining. For staining cells were incubated in 3.3% of Lysotracker intermediate solution and 0.05 % MitoTracker Red dye in cell growth medium at 37°C for 15 minutes. Cells were rinsed with pre-warmed 1× PBS for 3 times and imaged immediately in 1 ml of 1× PBS. Cells were imaged with a laser scanning confocal microscope LSM 780 (Zeiss). Images were acquired with a Zeiss C-Apochromat 63×/1.20 W Korr water immersion objective using ZEN software. Zoom level was set to 1.0.

3.4 Conventional Transmission Electron Microscopy (TEM)

Electron microscopy sample fixation was done as in (Ban-Ishihara et al., 2013). Confluent cells at 80-100% in 100 ml culture dish were rinsed with 2 ml 1 × PBS. Then 10 ml of 2%

glutaraldehyde + 2% paraformaldehyde in 1 × PBS solution was added to each dish with cells and incubated for 30 minutes at 4˚C and transferred to 2% glutaraldehyde in PBS at room temperature. Next the first fixation media was removed and 10 ml of 2 % glutaraldehyde in 1 × PBS was added to each dish. Fixed cells were stored at 4˚C until transported to EM laboratory. Cells were embedded, and blocks cut into thin sections, stained and prepared with OsO_4 reagent according to the standard procedure of the Laboratory of Electron Microscopy, University of Turku, Finland as described in detail on Appendix 8.1. Grids were imaged with a JEOL JEM-1400 plus transmission electron microscope equipped with an 11 Mpx Olympus Quemesa digital camera.

3.5 Immuno Transmission Electron Microscopy (Immuno-TEM)

3.5.1 Pre-embedding immunolabelling

Incubation with antibodies were performed in a moist chamber, with cells facing down where small dropplets of primary antibody (10-20 µl) and secondary antibody (20-30 µl) were added. Sample was fixed with PLP-fixative for 2 hours at room temperature. Next, sample was washed 3 times with 0.1 $Na\text{-}PO_4$ for 5 minutes at pH 7.4. Cells were permebialized with Saponin from Quillaja Bark, Sigma S-7900 for 8 minutes. Sample was incubated with primary anti-GFP antibody (mouse monoclonal) diluted 1:50 to Saponin from Quillaja Bark, Sigma S-7900 for 1 hour in moist chamber at room temperature. Next, sample was washed 3 times with Saponin from Quillaja Bark, Sigma S-7900 for 5 minutes. Sample was incubated with Nano-gold anit-Mouse IgG secondary antibody diluted 1:60 to Saponin from Quillaja Bark, Sigma S-7900 for 1 hour in moist chamber at room temperature. Sample was washed 3 times with Saponin from Quillaja Bark, Sigma S-7900 for 5 minutes. Next, sample was washed 3 times with $NA\text{-}PO_4$ for 5 minutes. Sample was exposed to post-fixation with 1% glutaraldehyde in $Na\text{-}PO_4$ for 5 minutes. Then, sample was washed once with $Na\text{-}PO_4$ for 5 minutes, and further quenched with 50mM Glycine in $Na\text{-}PO_4$ for 5 minutes. Next, sample was washed 3 times with $Na\text{-}PO_4$ for 3 minutes. Sample was washed 3 times with DW for 3 minutes.

3.5.2 Silver enhancement

Silver enhancement procedure is reported to give significantly higher densities of silver-enhanced gold nanoparticles than other methods (Tanner, Ploug, and Tao-Cheng 1996). Given that reactants were light sensitive, silver enhancement protocol was performed under minimal light conditions with infrared light at room temperature. A mixture of 200 µl initiator, 200 µl moderator and 200 µl activator was prepared as indicated by manufacter specifications (HQ silver enhancement kit, nanoprobes). Samples were exposed to mixture for 1, 3, 5 and 10 minutes according to the calibration. Next, samples were washed twice with DW for 5 minutes to stop the reaction. For gold toning, samples were exposed as follows:

2% Na Acetate 3 times for minutes at room temperature.

0.05% $HAuCl_4$ for 10 minutes on ice.

0.3% $Na_2S_2O_3$ twice for 10 minutes on ice.

Then, samples were washed 3 times with DW for 3 minutes. Then, samples were submitted to osmication, dehydration and Epon-embedding proccedures as indicated in Appendix 8.2 Embedding monolayers in Epon, omitting step 1 and 2.

3.6 Correlative light and electron microscopy with live cell imaging (CLEM)

Cells were seeded on 35 mm gridded glass bottom dishes coated with polylysine and cultured, synchronized and stained with MitoTracker Orange and LysoTracker Blue as described above. Cells were rinsed and kept in FluoroBrite DMEM (without phenol-red) during imaging. Live confocal imaging was performed with a Zeiss LSM 780 Laser Scanning Confocal Microscope (Carl Zeiss SAS, Jena, Germany) with a Plan-Apochromat 20.0x 0.8 air objective, excitation lasers line of 405 nm and 561 were selected for LysoTracker Blue and MitoTracker Orange respectively. The plate was mounted on a temperature-controlled incubation chamber. The locations of imaging were marked after acquisition. Immediately after imaging, the cells were washed with PBS, and fixed with 5% glutaraldehyde in PBS overnight at room temperature. Cells were embedded according to the optimized CLEM protocol of the Laboratory of Electron Microscopy, University of Turku, Finland (Prabhakar et al. 2018). Embedded blocks were held in place with a metal clip to ensure the specific location for CLEM was obtained. Ultrathin section of 60 nm thickness was cut with an ultramicrotome (Leica Microsystems, Germany), and sections were placed on copper O-rings to maximize the area of observation. Transmission

electron microscopy (TEM) images were obtained by using JEM 1400-Plus (JEOL, Japan) instrument at a 120-kV acceleration voltage.

3.7 Immunofluorescence

Cells were grown on glass coverslips, fixed with 3.7% PFA for 5 mins at room temperature, and permeabilized with 0.1% Triton X-100 at room temperature. Blocking was carried out with 1% BSA for in PBS for 1 h at room temperature. Coverslips were incubated with primary antibody in blocking solution at +4 ºC overnight. Coverslips were washed three times in PBS and then incubated with an appropriated conjugated secondary antibody, followed by two washes in PBS, one wash in MiliQ-H2O and mounting with mowiol.

3.8 Image analysis

Microscopy Image Browser (MIB) software (Belevich et al. 2016), an open-source image analysis software specially design for EM imaginary, was requested for testing (Supplementary License) and used to attempt analyze EM images.

4. Results

4.1 Transmission electron microscopy and correlative light electron microscopy imaging of vesicles-like structures positive to mitotracker and lysotracker

Mitochondrial integrity represents a fundamental element for cell survival. However, in order to fulfill their main function in an efficient manner, that is energy production, mitochondria constantly produce reactive oxygen species (ROS). ROS are highly toxic when accumulated, which implicates that their control is critical for mitochondrial homeostasis. Given that Mitochondrial complex I is one of the main sources of superoxide ROS control over complex I, it is just as essential for mitochondrial homeostasis.

In order to investigate mitochondrial response to ROS stress and its role on mitochondrial degradation, we allotropically induced the expression of alternative respiratory enzymes on human cells. Cells were further embedded and blocks were cut into thin sections and stained with OsO4 according to the standard procedure of the Laboratory of Electron Microscopy, University of Turku, Finland as described in detail in Appendix 8.1. The grids were imaged with a JEOL JEM-1400 plus transmission electron microscope equipped with an 11 Mpx Olympus Quemesa digital camera.

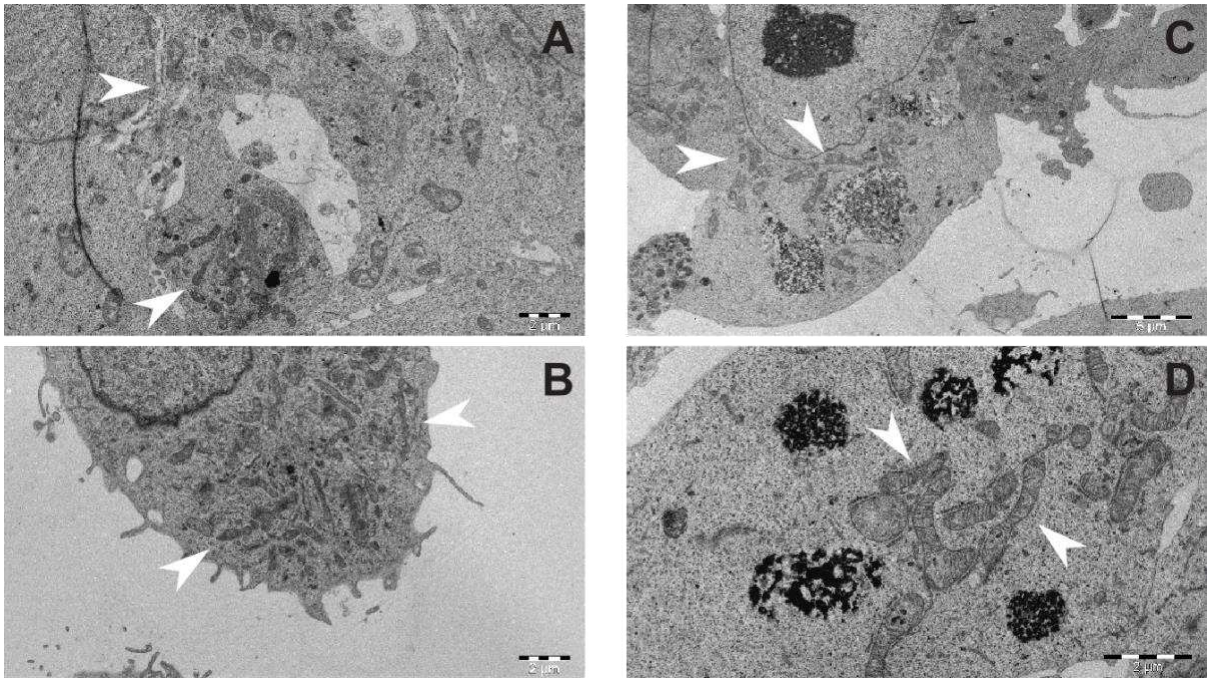

Figure 3. **Simple Transmission Electron Microscopy of human cells allotropically expressing NADH-ubiquinone oxidoreductase chain 1 (NDI1)**. Panels **A**-**B** depict control cellular culture, whereas panels **C**-**D** show cell cultures where NDI1 has been allotropically altered. As a consequence, qualitative morphological differences as well as an increased number of vesicle-like structures, indicated by arrow heads, can be observed.

I collected a total of 177 images at random, 135 of which were cases and 42 controls, where I observed qualitative differences in terms of number and morphology of subcellular vesicle-like structures, as depicted in **Figure 3** and described below.

Differences in morphology and number of mitochondria can be observed in the sample images above. These patterns persist in the remanding of the dataset (177 images), which is not shown. Control cells display round-like mitochondria with harmonious-shaped mitochondrial cristae. In contrast, allotropically-altered NDI1 cells show more numerous mitochondria that arrange confluent to each other as well as harbor irregular-shaped mitochondrial inner membrane protrusions.

Microscopy Image Browser (MIB), developed and licensed by University of Helsinki, was requested for the purpose of automated image analysis, i.e., image segmentation of mitochondriae and vesicle-like structures, and further quantification. However, image

segmentation and quantification were attempted with little success for a variety of reasons, including due to the characteristics of the images, i.e., low contrast.

Even for this relatively small dataset, manual segmentation, quantification and other kinds of image processing and analysis impose significant barriers. Not only due to the amount of work they would represent, but also because the possibility of introducing errors and biases. Approaches on image processing have been developed lately with the artificial intelligence revolution, for instance convolutional neural networks. Such approaches promise not only to function on high contrast imaging, namely fluorescence or reporter-based imaging, but also on low contrast and feature intensive imaging, such as electron microscopy. Moreover, these techniques are portable and easily scalable to large datasets. None of such techniques were used nor considered as alternatives for image analysis during this thesis.

Mitochondrial degradation pathways are not yet fully understood. Previous reports indicate that vesicle-like structures, which are positive for mitotracker and lysotracker, are transferred among neighboring cells (Davis et al. 2014; Davis and Marsh-Armstrong 2014). Nevertheless, the ultimate purpose of these events remains unclear.

To further investigate the nature of these vesicle-like structures in these experiments and obtain high-resolution images, I carried out a series of tests with the goal of establishing experimental parameters on the fluorescence imaging section of CLEM as depicted in **Figure 4**.

The results from these experiments are important for a number of reasons. First, these results form part of a larger project aimed at understanding mitochondrial degradation recently described by the process, transmitophagy. Conventional TEM of cells allotropically expressing NDI1 captures morphological differences in a mitochondrial cycle as shown in Figure 4, i.e., degradation, when ROS equilibrium is altered (Radi 2018). Moreover, experimental tests for CLEM should help in establishing parameters for further observations.

Combination of fluorescence imaging, where cells can be alive and reporters can be introduced, and electron microscopy, where cells have been imaged at a higher resolution at the cost of being fixed and embedded for a long period of time. Super resolution techniques, either deterministic, such as STED, or stochastic, such as STORM, offer more resolution that conventional confocal microscopy. However, these techniques are likewise dependent on reporters, which limits the observational space to unexpected features.

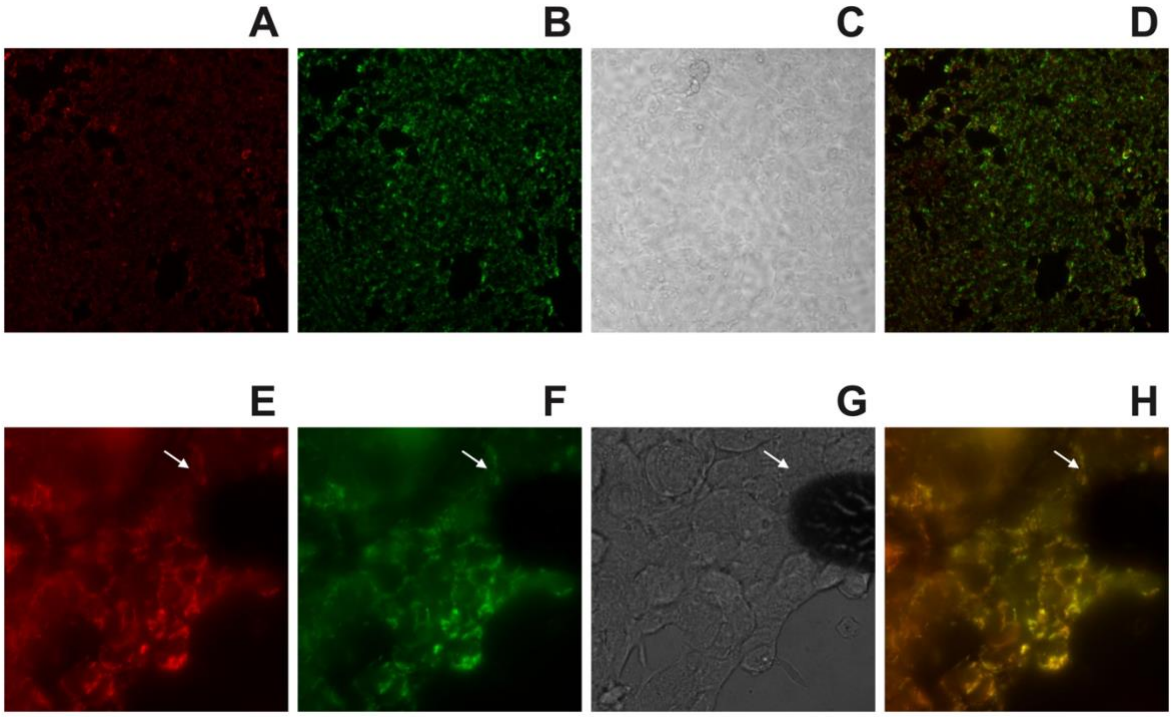

Figure 4. **Cell culture with Mitotracker and Lysotracker confocal fluorescent staining**. Panel **A**, **B** and **C** depict confocal fluorescent staining for Lysotracker (panel A) and Mitotracker (panel B) as well as bright field. Panel **D** shows both fluorescent signals. Likewise, panels **E**, **F**,and **G** display confocal flourescent statining for Lysotracker (panel E) and Mitotracker (panel F) and bright field (panel G) with gold nanoparticle ink printed coverslip, as indicated by arrow, to perform Conventional Transmission Electron Microscopy. Panel **H** shows both flourescent signals.

4.2 Fluorescence and immuno electron microscopy imaging of nucleoids at ER-mitochondrial contact sites

ER interactions with mitochondria are essential for several cellular processes, such as calcium intracellular homeostasis, lipid metabolism and mitochondrial DNA maintenance, to name a few. These interactions occur at MAMs, which are complexes characterized by lipid rich contact sites. Some proteins have been identified to be abundant in such structures. Biochemistry experimental data indicates that Twinkle helicase, a protein responsible for mtDNA replication, is enriched at MAM (Gerhold, Cansiz-Arda et al. 2015). However, spatial information is yet lacking to understand how, when and where these interactions occur.

To identify the presence of Twinkle helicase and FACL4, a marker for MAM, and analyze their morphology on mitochondrial membrane, I prepared cell cultures and immunolabeled Twinkle helicase and FACL4, and further imaged with confocal fluorescent microscopy as well as with super resolution microscopy techniques, namely stimulated emission depletion (STED) microscopy.

In our initial experiments, we were able to capture adequate fluorescent signal during confocal microscopy, data not shown, as well as during STED microscopy from Twinkle and FACL4 staining as shown in **Figure 5**. Qualitative observations confirm colocalization, however replicates and quantitative data is still needed to corroborate these investigations.

Fluorescence staining responds well to labeling during high resolution imaging. FACL4, a marker for MAM is properly depicted in Figure 5 panel A where it is expected to observe mitochondrial contact sites. Likewise, Twinkle helicase is presented on Figure 5 panel B. Figure 5 panel C presents over position of both previous panels where it is possible to observe fluorescence red signals overlapping with fluorescence green signals, as previously described.

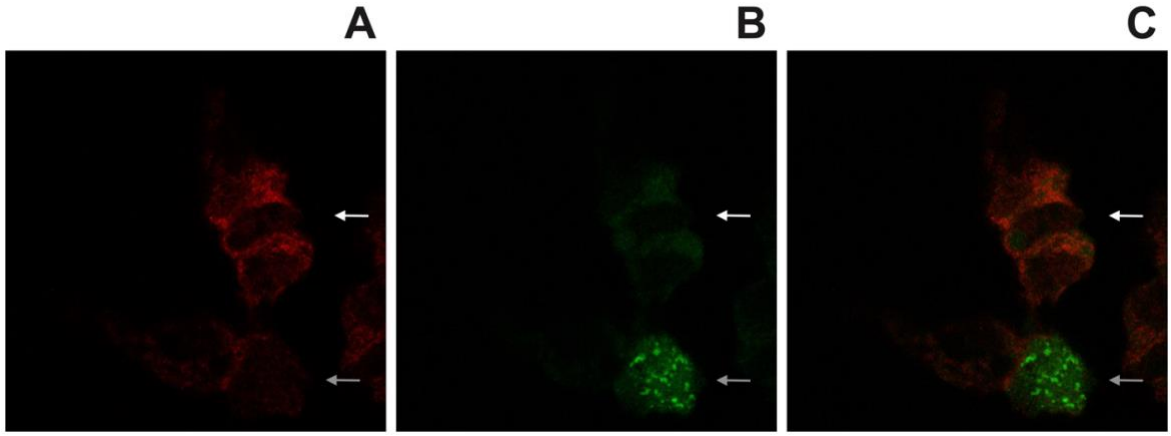

Figure 5. Super resolution fluorescence microscopy STED of Twinkle helicase and FACL4, a marker for MAM. Images show fluorescent signals for and FACL4 (panel A) and Twinkle helicase (panel B). Panel C depicts qualitative colocalization between fluorescent targets, as illustrated by white arrow. Gray arrow at the bottom right of panel C, indicates qualitive presence of Twinkle helicase (green flourophore), but absence of FACL4 (red flourophore).

ATAD3 is present in mitochondrial nucleoids, which partake of mitochondrial DNA replication. Biochemistry evidence suggests that ATAD3 is a membrane protein that holds together membrane structures at the nucleoid-MAM contact sites. In order to study the nucleoid-MAM association in depth, we performed a series of tests where ATAD3 was knocked-down and collected high-resolution images, i.e., immuno TEM. Usually, immuno TEM involves the usage of antibodies against a specific target labelled with gold particles. The gold is used to create a high contrast image due to its high density. A technical challenge when working with mitochondria, which harbor a double membrane, is to internalize the gold particles properly. To overcome this issue, I exposed knock-down ATAD3 samples to silver coating for different times previous to gold particle labelling.

The aim of this experiment was to optimize the technique by localizing ATAD3 on the membrane as well as to examine FACL4 and Twinkle presence after the nucleoid-MAM connection has been disrupted by ATAD knock-down. Such results could help with 3D reconstructions on future experiments. Such experiments were carried out but I did not partake on them.

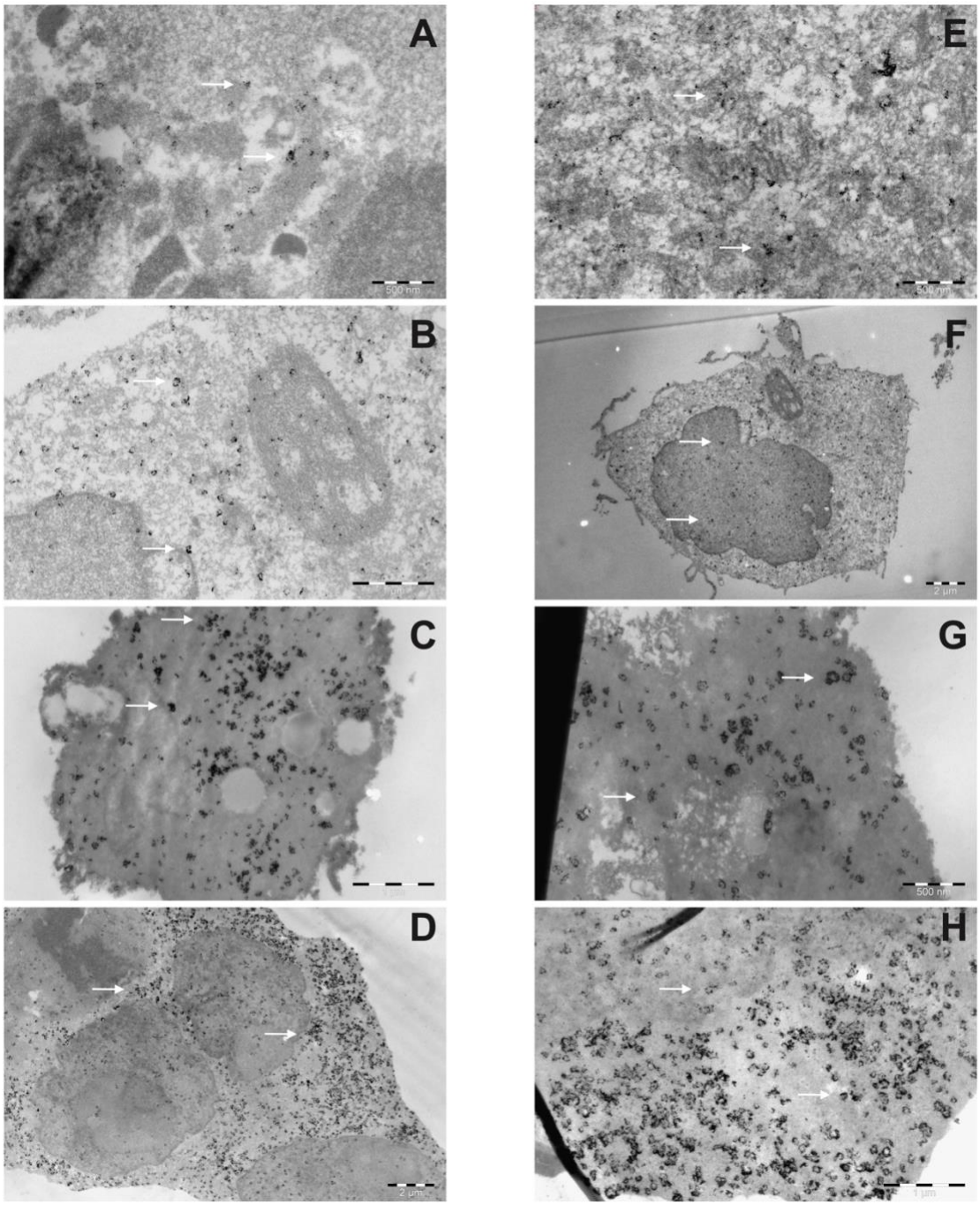

Figure 6. Immuno TEM time series. Exposition to silver coating at 1 (panels A and E), 3 (panels B and F), 5 (panels C and G) and 10 (panels D and H) minutes. Arrows indicate binding of immunological targets by gold conjugated antibodies (non-exhaustive annotation).

I tested different exposition times to silver coating in our ATAD3 had been knocked-down **s**amples previous to standard gold labelling and TEM preparation as indicated in **Figure 6**. Qualitative observations indicated the utility of silver enhancement after to nano gold labelling and followed by gold chemical stabilization for imaging cellular structures enclosed by membranes, such as mitochondria. These results set up experimental conditions for studying ER - mitochondrial contact sites interactions by different imaging techniques.

Different exposition times to silver coating allow for different penetration in cell structures. As such these differences are presented in Figure 6, where short incubations times, e.g., 1 minute of incubation for silver coating on Figure 6 panels A and E produce dim signals on TEM, whereas long incubations times, e.g., 10 minutes of incubation for silver coating on Figure 6 panels D and H produce stronger signals at the cost of introducing potential noise. Intermediary incubation times, e.g., incubation of 3 and 5 minutes for silver coating as displayed on Figure 6 panels B and F and C and G, respectively, present alternatives to balance signal to noise ratio. Although these experiments are not conclusive, they set up an advantageous platform for further experimentation for several reasons, such as: they prove that the incubation times with silver coating change the deposition of silver and therefore influence directly the signal to noise ratio during TEM; they show that proper labeling of mitochondrial protein target is possible and effect, which is particularly interesting and relevant given the physiology and morphology of mitochondria in relation to the cell, i.e., intracellular organelle with a double lipid layer.

5. Discussion

5.1 Mitochondrial degradation

Mitochondria turnover has been conceived in terms of biogenesis and degradation by means of mitophagy or apoptosis. These two pathways are critical for the life cycle of cells. Mitochondria are heavily involved in both of these processes, therefore involved in the fate of cells. Apart from this, a new pathway for mitochondrial degradation has been observed in cells with extremely large cytoplasm and cellular membrane, i.e., neurons (Davis et al. 2014; Davis and Marsh-Armstrong 2014), where mitochondria become engulfed in vesicles and transported to neighboring cells.

Studying this process of mitochondrial degradation is important because of its presumed role in a variety of diseases, most prominently neurodegenerative diseases (Leal and Martins 2021). Since neurons have a larger cellular body size than other cells, cytoplasmic events are carried out more extremely, therefore have a much larger effect and can be more likely observed. Moreover, mitophagy has also been suggested to play a role in other diseases related to aging (Shi, Guberman, and Kirshenbaum 2018) and diabetes type 2 (Rovira-Llopis et al. 2017). These observations emphasize the importance and dynamics of mitochondrial physiology, expect in cardiomyocytes where they tend to be static (Shirihai, Song, and Dorn 2015).

To study these phenomena in detail, an increased redox stress state in cell cultures was induced by suppressing the expression of NDI1. This leads to the accumulation of redox byproducts, particularly superoxide (Radi 2018). This translate into more likely observable degradation events at a given timepoint, which was captured with different methods in this project.

In this manner, a simulated biological conditions where mitochondrial degradation is more probable to occur was created. Next, electron microscopy was performed to capture the ultra-structure at the time when events were occurring. In our preliminary experiments, vesicle-like structures, which resemble mitochondria both morphological and biochemically, were observed. However, no observations of mitochondria being transferred through cell-to-cell contacts were possible. Had such phenomena been present, they could have been suggestive of

the new mitochondrial degradation pathway as it has been observed in neurons (Davis et al. 2014; Davis and Marsh-Armstrong 2014). Nevertheless, according to the current observations, I can only conclude that morphological changes occur under ROS stress.

Although, TEM provides good quality resolution images, it lacks functional and physiological aspects, in other words, TEM can only capture static images. To investigate this problem further, an the experimental set up that included a functional aspect by combining labelling with fluorophores with the high-detailed images was explored. Thus, labeled mitochondrial vesicles with MitoTracker and lysosome vesicles with LysoTracker were mounted on a gold nanoparticle ink printed coverslip, captured fluorescence microscopy imagery and proceeded with transmission electron microscopy imaging. In this manner, an experimental set up to attempt to corroborate that the morphologically compatible vesicles was layed out. This is experimental set up was critical due to the fact that such vesicles had been observed in previous experiments, and succesfully observing them with the biochemical profile of degradative organelles could connect the ultra-structure with the physioilogical condition.

Automatic image processing of the electron microscopy data, that is image segmentation and quantification, failed. Such unsuccessful attempt can be explained by the lack of substantial contrast in the data as well as image processing heavily reliant on manual operation. Other alternatives that strive on different segmentation and quantification methods might be more appropriate both for this dataset as well as expandable to a wide variety microscopy dataset, e.g., convolutional neural networks or other types of unsupervised artificial intelligence. Moreover, extended experience and aquantaince with electron microscopy imagery is required to perform adecuate image segmentation and processing in such a manual intensive manner. This means that methods that do not enterly rely on manual operation could introduce less baises and therefore could be potentially more beneficial to use, even for small datasets such as the dataset collected and presented on this thesis.

Although more data is required to establish solid conclusions, I have established adequate and replicable experimental parameters. Much is yet to be discovered about this pathway and its implications for health and disease.

5.2 Mitochondrial nucleoids

The idea of cells organelles being independent entities tasked with a few isolated functions has been proven wrong. Nowadays, it is widely accepted that intracellular organelles are tethered together, both physically and physiological, to fulfill the demands of the cell. This idea encompasses mitochondria as well, which nevertheless in certain aspects retain their independent physiology. As such, mitochondria interact tightly with ER. These interactions are essential for cell homeostasis. Beyond all previously known knowledge, proteins involved in mtDNA replication are suspected to associate tightly with ER-mitochondrial junctions (Ježek et al. 2019; Spelbrink 2009).

These ER-mitochondrial junctions are orchestrated by a sub-set of nucleoids. The biochemical profile of these nucleoids is defined by the presence of the protein Twinkle helicase. During this project, I attempted to collect images that proves the presence of Twinkle helicase in close proximity to MAMs, which are in turn defined by the presence of FACL4. ATAD3 is found at the center of this interaction (Rajala et al. 2014; Gerhold et al. 2015). As such, it has been observed that mutations on ATAD3 can lead to mitochondrial genetic diseases (Murayama et al. 2019). Moreover, previous results indicate that knock-down of ATAD3 by RNAi leads to changes in mitochondrial cristae morphology, which implies the fundamental role of ATAD3 as a membrane protein that likely holds together membrane structures at the nucleoid-MAM contact sites.

To investigate the association of Twinkle helicase and MAMs, I collected high-resolution images through different methods, such as confocal, super resolution and electron microscopy. First, I used fluorochrome labelling to co-localize TWN and FALC4. Together with previous biochemical evidence, this demonstrates the spatial association between replicative nucleoids and MAMs. Next, 3D reconstructions of mitochondrial membranes from TEM images were created. Furthermore, I tested and established experimental conditions using an immuno labelling protocol with silver staining and nano-gold particles to locate mitochondrial proteins during TEM.

Understanding mitochondrial physiology, in this case mitochondrial DNA replication, is important. Mitochondrial are indispensable actors in cellular physiology in eukaryote organisms. The disruption of mitochondrial pathways has previously been linked to

pathological states. The data collected during these experiments focuses on providing spatial information about the interactions among different components involved in mitochondrial DNA replication as well as circumstances where these components are disrupted.

6. Acknowledgments

The work presented in this thesis was carried out between February 2015 and August 2015 at the Laboratory of Electron Microscopy, University of Turku, Finland and Laboratory of Lipid and Membrane Research, Abo Akademi, Finland.

I would like to thank Nathaniel Street for his supervision and guidance on writing this thesis. I would also like to thank Helen Cooper, Markus Peurla and Eric Dufour who were responsible for planning and supervising the experimental part of this thesis. Credit goes also to the Biomedical Imaging program coordinators for all their hard work and all people at the imaging facilities.

Lastly, but certainly not less importantly, I would like to thank all people involved directly or indirectly in previous research, being involved in the field of mitochondria, in the technology development or simply paying taxes to fund research, that allowed this project to take place. It is only step-by-step that we can pushed our limits a little bit further.

7. References

Anderson, Sarah R., David Parmiter, Ulrich Baxa, and Kunio Nagashima. 2018. 'Immunoelectron Microscopy for Visualization of Nanoparticles.' in (Springer New York).

Ashrafi, G., and T. L. Schwarz. 2013. 'The pathways of mitophagy for quality control and clearance of mitochondria', *Cell Death & Differentiation*, 20: 31-42.

Babior, B. M. 2004. 'NADPH oxidase', *Curr Opin Immunol*, 16: 42-7.

Bates, Mark, Bo Huang, Graham T. Dempsey, and Xiaowei Zhuang. 2007. 'Multicolor Super-Resolution Imaging with Photo-Switchable Fluorescent Probes', *Science*, 317: 1749-53.

Baudier, Jacques. 2018. 'ATAD3 proteins: brokers of a mitochondria-endoplasmic reticulum connection in mammalian cells', *Biological Reviews*, 93: 827-44.

Belevich, Ilya, Merja Joensuu, Darshan Kumar, Helena Vihinen, and Eija Jokitalo. 2016. 'Microscopy Image Browser: A Platform for Segmentation and Analysis of Multidimensional Datasets', *PLOS Biology*, 14: e1002340.

Boveris, Alberto, and Enrique Cadenas. 1975. 'Mitochondrial production of superoxide anions and its relationship to the antimycin insensitive respiration', *FEBS Letters*, 54: 311-14.

Braga, Patrícia C., Marco G. Alves, Anabela S. Rodrigues, and Pedro F. Oliveira. 2022. 'Mitochondrial Pathophysiology on Chronic Kidney Disease', *International Journal of Molecular Sciences*, 23: 1776.

Cairns, George, Madhavee Thumiah-Mootoo, Yan Burelle, and Mireille Khacho. 2020. 'Mitophagy: A New Player in Stem Cell Biology', *Biology*, 9: 481.

Cogliati, Sara, Jose A. Enriquez, and Luca Scorrano. 2016. 'Mitochondrial Cristae: Where Beauty Meets Functionality', *Trends in Biochemical Sciences*, 41: 261-73.

Dang, Quynh-Chi L., Duong H. Phan, Abigail N. Johnson, Mukund Pasapuleti, Hind A. Alkhaldi, Fang Zhang, and Steven B. Vik. 2020. 'Analysis of Human Mutations in the Supernumerary Subunits of Complex I', *Life*, 10: 296.

Davis, Chung-Ha O., Keun-Young Kim, Eric A. Bushong, Elizabeth A. Mills, Daniela Boassa, Tiffany Shih, Mira Kinebuchi, Sebastien Phan, Yi Zhou, Nathan A. Bihlmeyer, Judy V. Nguyen, Yunju Jin, Mark H. Ellisman, and Nicholas Marsh-Armstrong. 2014. 'Transcellular degradation of axonal mitochondria', *Proceedings of the National Academy of Sciences*, 111: 9633-38.

Davis, Chung-Ha O., and Nicholas Marsh-Armstrong. 2014. 'Discovery and implications of transcellular mitophagy', *Autophagy*, 10: 2383-84.

Dinicolantonio, James J., Mark F. McCarty, and James H. O'Keefe. 2022. 'Coenzyme Q10 deficiency can be expected to compromise Sirt1 activity', *Open Heart*, 9: e001927.

Frey, Terrence G., and Carmen A. Mannella. 2000. 'The internal structure of mitochondria', *Trends in Biochemical Sciences*, 25: 319-24.

Gerhold, Joachim M., Şirin Cansiz-Arda, Madis Lõhmus, Oskar Engberg, Aurelio Reyes, Helga Van Rennes, Alberto Sanz, Ian J. Holt, Helen M. Cooper, and Johannes N. Spelbrink. 2015. 'Human Mitochondrial DNA-Protein Complexes Attach to a Cholesterol-Rich Membrane Structure', 5: 15292.

Giacomello, Marta, Aswin Pyakurel, Christina Glytsou, and Luca Scorrano. 2020. 'The cell biology of mitochondrial membrane dynamics', *Nature Reviews Molecular Cell Biology*, 21: 204-24.

Hell, S. W., and J. Wichmann. 1994. 'Breaking the diffraction resolution limit by stimulated emission: stimulated-emission-depletion fluorescence microscopy', *Opt Lett*, 19: 780-2.

Hell, Stefan W. 2003. 'Toward fluorescence nanoscopy', *Nature Biotechnology*, 21: 1347-55.

Horvath, Susanne E., and Günther Daum. 2013. 'Lipids of mitochondria', *Progress in Lipid Research*, 52: 590-614.

Huang, Bo, Sara A. Jones, Boerries Brandenburg, and Xiaowei Zhuang. 2008. 'Whole-cell 3D STORM reveals interactions between cellular structures with nanometer-scale resolution', *Nature Methods*, 5: 1047-52.

Ikon, N., and R. O. Ryan. 2017. 'Cardiolipin and mitochondrial cristae organization', *Biochim Biophys Acta Biomembr*, 1859: 1156-63.

Ježek, Petr, Tomáš Špaček, Jan Tauber, and Vojtěch Pavluch. 2019. 'Mitochondrial Nucleoids: Superresolution microscopy analysis', *The International Journal of Biochemistry & Cell Biology*, 106: 21-25.

Kubli, Dieter A., and Åsa B. Gustafsson. 2012. 'Mitochondria and Mitophagy', *Circulation Research*, 111: 1208-21.

Leal, Nuno Santos, and Luís Miguel Martins. 2021. "Mind the Gap: Mitochondria and the Endoplasmic Reticulum in Neurodegenerative Diseases." In *Biomedicines*, 227. MDPI AG.

Lee, Hsiao-Lu D., Samuel J. Lord, Shigeki Iwanaga, Ke Zhan, Hexin Xie, Jarrod C. Williams, Hui Wang, Grant R. Bowman, Erin D. Goley, Lucy Shapiro, Robert J. Twieg, Jianghong Rao, and W. E. Moerner. 2010. 'Superresolution Imaging of Targeted Proteins in Fixed and Living Cells Using Photoactivatable Organic Fluorophores', *Journal of the American Chemical Society*, 132: 15099-101.

Loschen, Gerriet, Angelo Azzi, Christoph Richter, and Leopold Flohé. 1974. 'Superoxide radicals as precursors of mitochondrial hydrogen peroxide', *FEBS Letters*, 42: 68-72.

Małecki, Jędrzej M., Erna Davydova, and Pål Ø Falnes. 2022. 'Protein methylation in mitochondria', *Journal of Biological Chemistry*, 298: 101791.

Melser, Su, Julie Lavie, and Giovanni Bénard. 2015. 'Mitochondrial degradation and energy metabolism', *Biochimica et Biophysica Acta (BBA) - Molecular Cell Research*, 1853: 2812-21.

Merle, N., O. Feraud, B. Gilquin, A. Hubstenberger, S. Kieffer-Jacquinot, N. Assard, A. Bennaceur-Griscelli, J. Honnorat, and J. Baudier. 2012. 'ATAD3B is a human embryonic stem cell specific mitochondrial protein, re-expressed in cancer cells, that functions as dominant negative for the ubiquitous ATAD3A', *Mitochondrion*, 12: 441-8.

Murayama, K., M. Shimura, Z. Liu, Y. Okazaki, and A. Ohtake. 2019. 'Recent topics: the diagnosis, molecular genesis, and treatment of mitochondrial diseases', *J Hum Genet*, 64: 113-25.

Ni, Hong-Min, Jessica A. Williams, and Wen-Xing Ding. 2015. 'Mitochondrial dynamics and mitochondrial quality control', *Redox Biology*, 4: 6-13.

Okamoto, Koji. 2011. 'Mitochondria breathe for autophagy', *The EMBO Journal*, 30: 2095-96.

Okamoto, Koji, and Noriko Kondo-Okamoto. 2012. 'Mitochondria and autophagy: Critical interplay between the two homeostats', 1820: 595-600.

Parey, K., C. Wirth, J. Vonck, and V. Zickermann. 2020. 'Respiratory complex I - structure, mechanism and evolution', *Curr Opin Struct Biol*, 63: 1-9.

Patterson, George H. 2009. 'Fluorescence microscopy below the diffraction limit', *Seminars in Cell & Developmental Biology*, 20: 886-93.

Pepe, Salvatore, Robert M. Mentzer, and Roberta A. Gottlieb. 2014. 'Cell-permeable protein therapy for complex I dysfunction', *Journal of Bioenergetics and Biomembranes*, 46: 337-45.

Pereira, Guilherme Augusto Reissig, and Luís Beck-Da-Silva. 2022. 'Deficiência de Ferro na Insuficiência Cardíaca com Fração de Ejeção Reduzida: Fisiopatologia, Diagnóstico e Tratamento', *Arquivos Brasileiros de Cardiologia*, 118: 646-54.

Plucinska, G., and T. Misgeld. 2016. 'Imaging of neuronal mitochondria in situ', *Curr Opin Neurobiol*, 39: 152-63.

Prabhakar, Neeraj, Markus Peurla, Sami Koho, Takahiro Deguchi, Tuomas Näreoja, Huan-Cheng Chang, Jessica M. Rosenholm, and Pekka E. Hänninen. 2018. 'STED-TEM Correlative Microscopy Leveraging Nanodiamonds as Intracellular Dual-Contrast Markers', *Small*, 14: 1701807.

Radi, Rafael. 2018. 'Oxygen radicals, nitric oxide, and peroxynitrite: Redox pathways in molecular medicine', *Proceedings of the National Academy of Sciences*, 115: 5839-48.

Rajala, N., J. M. Gerhold, P. Martinsson, A. Klymov, and J. N. Spelbrink. 2014. 'Replication factors transiently associate with mtDNA at the mitochondrial inner membrane to facilitate replication', *Nucleic Acids Res*, 42: 952-67.

Rovira-Llopis, S., C. Banuls, N. Diaz-Morales, A. Hernandez-Mijares, M. Rocha, and V. M. Victor. 2017. 'Mitochondrial dynamics in type 2 diabetes: Pathophysiological implications', *Redox Biol*, 11: 637-45.

Saravanan, Sanjana, Caitlin J. Lewis, Bhavna Dixit, Matthew S. O'Connor, Alexandra Stolzing, and Amutha Boominathan. 2022. 'The Mitochondrial Genome in Aging and Disease and the Future of Mitochondrial Therapeutics', *Biomedicines*, 10: 490.

Seo, Byoung Boo, Mathieu Marella, Takao Yagi, and Akemi Matsuno-Yagi. 2006. 'The single subunit NADH dehydrogenase reduces generation of reactive oxygen species from complex I', *FEBS Letters*, 580: 6105-08.

Shi, R., M. Guberman, and L. A. Kirshenbaum. 2018. 'Mitochondrial quality control: The role of mitophagy in aging', *Trends Cardiovasc Med*, 28: 246-60.

Shirihai, Orian S., Moshi Song, and Gerald W. Dorn. 2015. 'How Mitochondrial Dynamism Orchestrates Mitophagy', *Circulation Research*, 116: 1835-49.

Spelbrink, J. N., F. Y. Li, V. Tiranti, K. Nikali, Q. P. Yuan, M. Tariq, S. Wanrooij, N. Garrido, G. Comi, L. Morandi, L. Santoro, A. Toscano, G. M. Fabrizi, H. Somer, R. Croxen, D. Beeson, J. Poulton, A. Suomalainen, H. T. Jacobs, M. Zeviani, and C. Larsson. 2001. 'Human mitochondrial DNA deletions associated with mutations in the gene encoding Twinkle, a phage T7 gene 4-like protein localized in mitochondria', *Nat Genet*, 28: 223-31.

Spelbrink, Johannes N. 2009. 'Functional organization of mammalian mitochondrial DNA in nucleoids: History, recent developments, and future challenges': n/a-n/a.

Stockert, Juan Carlos; Blazquez-Castro, Alfonso 2017. 'Fluorescence Microscopy in Life Sciences', *Bentham Science Publishers*.

Stotland, Aleksandr, and Roberta A. Gottlieb. 2015. 'Mitochondrial quality control: Easy come, easy go', *Biochimica et Biophysica Acta (BBA) - Molecular Cell Research*, 1853: 2802-11.

Szymański, Jędrzej, Justyna Janikiewicz, Bernadeta Michalska, Paulina Patalas-Krawczyk, Mariasole Perrone, Wiesław Ziółkowski, Jerzy Duszyński, Paolo Pinton, Agnieszka Dobrzyń, and Mariusz Więckowski. 2017. 'Interaction of Mitochondria with the Endoplasmic Reticulum and Plasma Membrane in Calcium Homeostasis, Lipid Trafficking and Mitochondrial Structure', *International Journal of Molecular Sciences*, 18: 1576.

Tam, Johnny, and David Merino. 2015. 'Stochastic optical reconstruction microscopy (STORM) in comparison with stimulated emission depletion (STED) and other imaging methods', *Journal of Neurochemistry*, 135: 643-58.

Tanner, V. A., T. Ploug, and J. H. Tao-Cheng. 1996. 'Subcellular localization of SV2 and other secretory vesicle components in PC12 cells by an efficient method of preembedding EM immunocytochemistry for cell cultures', *Journal of Histochemistry & Cytochemistry*, 44: 1481-88.

Tilokani, Lisa, Shun Nagashima, Vincent Paupe, and Julien Prudent. 2018. 'Mitochondrial dynamics: overview of molecular mechanisms', *Essays In Biochemistry*, 62: 341-60.

Tong, Mingming, and Junichi Sadoshima. 2016. 'Mitochondrial autophagy in cardiomyopathy', *Current Opinion in Genetics & Development*, 38: 8-15.

Usey, Madelaine M., and Diego Huet. 2022. 'Parasite Powerhouse: a Review of the Toxoplasma gondii Mitochondrion', *Journal of Eukaryotic Microbiology*.

Vance, Jean E. 2014. 'MAM (mitochondria-associated membranes) in mammalian cells: Lipids and beyond', *Biochimica et Biophysica Acta (BBA) - Molecular and Cell Biology of Lipids*, 1841: 595-609.

Vicidomini, Giuseppe, Paolo Bianchini, and Alberto Diaspro. 2018. 'STED super-resolved microscopy', *Nature Methods*, 15: 173-82.

Voortman, Lenard M. 2014. 'Integration Without Compromise', *Microscopy Today*, 22: 30-35.

Williams, M., and M. C. Caino. 2018. 'Mitochondrial Dynamics in Type 2 Diabetes and Cancer', *Front Endocrinol (Lausanne)*, 9: 211.

Yagi, Takao, Byoung Boo Seo, Salvatore Di Bernardo, Eiko Nakamaru-Ogiso, Mou-Chieh Kao, and Akemi Matsuno-Yagi. 2001. *Journal of Bioenergetics and Biomembranes*, 33: 233-42.

Young, Matthew J., and William C. Copeland. 2016. 'Human mitochondrial DNA replication machinery and disease', *Current Opinion in Genetics & Development*, 38: 52-62.

Zhang, Baoyi, Cunyao Pan, Chong Feng, Changqing Yan, Yijing Yu, Zhaoli Chen, Changjiang Guo, and Xinxing Wang. 2022. 'Role of mitochondrial reactive oxygen species in homeostasis regulation', *Redox Report*, 27: 45-52.

Zorzano, A., M. Liesa, and M. Palacin. 2009. 'Role of mitochondrial dynamics proteins in the pathophysiology of obesity and type 2 diabetes', *Int J Biochem Cell Biol*, 41: 1846-54.

8. Appendix

8.1 Specimen preparation for conventional transmission electron microscopy, Laboratory of Electron Microscopy, University of Turku.

1. Prefixation:
   5 % glutaraldehyde in 0.16 M s-collidin buffer, pH 7.4, at least 3 h.
2. 1st washes:
   rinse in s-collidin buffer 3 times, 3 min each.
3. Postfixation [Karnovsky, M.J. (1971), Proc. 11th Ann. Meet. Am. Soc. Cell Biol., New Orleans, p. 146a].
   2 % OsO4 + 3 % K-ferrocyanide (1:1) for 2 h
4. 2nd washes:
   rinse in distilled H2O 3 times, 5 min each.
5. Dehydration:
   - 70 % ethanol, 1 min at +4◦C.
   - 96 % ethanol, 1 min at +4◦C.
   - 100 % ethanol, 30 min at +4 ◦C.
   - 100 % ethanol, 3 times, 30 min each at +20 ◦C.
6. Embedding:
   - propylene oxide, 2 times, 15 min each.
   - propylene oxide + epoxy resin + DMP (10:10:0.2), 2 h.
   - epoxy resin + DMP (10:0.2), 12 h.
   - epoxy resin + DMP (10:0.2), +60 ◦C, 36 h.
7. Sectioning:
   The sections are cut with an ultramicrotome to a thickness of appr. 70 nm.
8. Uranyl acetate staining:
   Manual staining with 1 % uranyl acetate in 50 % EtOH for 30 min. Rinse in pure water 3 times, 30 s each.
9. Lead citrate staining:
   Manual staining with 0.3 % lead citrate in pure water for 3 min. Rinse in pure water 3 times, 30 s each.

8.2 Embedding monolayers in Epon.

1. Grow cells on glass coverslips, thickness #1 (0.13-0.16 mm).
2. Fix with 2% glutaraldehyde in 0.1 M NaCac or 0.1 M NaPO buffer at 7.4 pH for 20 - 30 minutes.
3. Wash twice with NaCac buffer for 3 minutes.
4. Osmicate for 1 hour with osmium from 2% OsO_4 in DW and 0.4 M NaCac buffer to final 1% OsO_4 in 0.1 M NaCac and added $K_4[Fe(CN)_6]$ 15 mg/ml.
5. Wash 2 times with 0.1 M NaCac buffer for 3 minutes.
6. Dehydrate as follows:
    a. Once with 70% EtOH.
    b. Once with 96% EtOH.
    c. Twice with absolute EtOH.
7. Dip coverslip with acetone, and place it onto an aluminum plate (on a plastic or aluminum dish/cover).
8. Without complete acetone evaporation, cover cells with Epon.
9. Place beem capsule filled with Epon upside down on top of the cells.
10. Incubate 2 hours at room temperature to allow Epon infiltration.
11. Incubate samples at 60ºC for 14 hours.
12. Transfer samples to coverslip. Alternatively, submerge samples on liquid-N_2.